A Novel Fatigue Assessment Approach by Direct Steady Cycle Analysis (DSCA) considering the temperature-dependent strain hardening effect

Xiaotao Zheng[1], Haofeng Chen[2*], Zhiyuan Ma[2], Fuzhen Xuan[3*]

1. Hubei Provincial Key Laboratory of Chemical Equipment Intensification and Intrinsic Safety, School of Mechanical and Electrical Engineering, Wuhan Institute of Technology, Wuhan 430205, P. R. China
2. University of Strathclyde,Glasgow, UK
3. Key Laboratory of Pressure System and Safety, MOE, School of Mechanical Engineering, East China University of Science and Technology, 130 Meilong Street, PO Box 402, Shanghai 200237, PR China

Abstract. The traditional Low Cycle Fatigue (LCF) evaluation method is based on elastic analysis with Neuber's rule which is usually considered to be over conservative. However, the effective strain range at the steady cycle should be calculated by detailed cycle-by-cycle analysis for the alternative elastic-plastic method in ASME VIII-2, which is obviously time-consuming. A Direct Steady Cycle Analysis (DSCA) method within the Linear Matching Method (LMM) framework is proposed to assess the fatigue life accurately and efficiently for components with arbitrary geometries and cyclic loads. Temperature-dependent stress-strain relationships considering the strain hardening described by the Ramberg-Osgood (RO) formula are discussed and compared with those results obtained by the Elastic-Perfectly Plastic (EPP) model. Additionally, a Reversed Plasticity Domain Method (RPDM) based on the shakedown and ratchet limit analysis method and the DSCA approach within the LMM framework (LMM DSCA) is recommended to design cyclic load levels of LCF experiments with predefined fatigue life ranges.

Keywords: Fatigue evaluation; Direct steady cycle analysis; Linear Matching Method; Ramberg-Osgood model; Temperature-dependent materials.

* Corresponding author: haofeng.chen@strath.ac.uk
* Corresponding author: fzxuan@ecust.edu.cn

1. Introduction

Fatigue is related to localized structural damage and cracking, which is considered as one of the most typical failure modes of process equipment, such as pressurized vessels and piping, under cyclic loads during the operating stage. Generally, fatigue can be categorized into LCF and High Cycle Fatigue (HCF) based on the fatigue life defined by number of cycles. HCF usually occurs when relatively low stresses are applied and the fatigue life is greater than 10^4 cycles. On the other hand, LCF fails in less than 10^4 cycles due to the cyclic loads are obviously higher and significant plastic deformation takes place at each cycle. It is reported that approximate 90% of all mechanical failures of metallic components are caused by fatigue [1]. Therefore, fatigue behaviors of metallic materials have been studied widely by fatigue testing [2], [3], [4], microscopic observation [5], [6], [7], lifetime prediction[8], [9], [10]. In order to avoid the fatigue failure of pressurized components, detailed fatigue assessment procedures are provided in design codes. The traditional LCF evaluation method to estimate the plastic strain range is based on the linear elastic analysis with the Neuber's rule. A linear elastic analysis is performed to obtain the elastic solution firstly, then a correction is made by the Neuber's rule considering the local plasticity to predict the strain ranges at stress concentration regions. Since this approach depends on the stress concentration and the induced strain range, the mechanical properties and local geometries influence the prediction accuracy significantly [11]. For example, it can be well used to predict the strain range for blunt notches under the plane stain condition [12], but may overestimate the local inelastic strains for sharp notches [13]. Until now, this approximate method has been used widely due to its safety, convenience and efficiency. However, it is usually considered to be over-conservative for the fatigue life assessment. As an alternative approach, the elastic-plastic method is also proposed in ASME VIII-2 [14]. According to this method, the steady effective strain range should be calculated using detailed non-linear cycle-by-cycle analysis. Although highly accurate local stress-strain relationships under arbitrary cyclic loads may be achieved, it is still computationally expensive and very impractical for those cases involving complex engineering structures and multiple load conditions. Accordingly, it is necessary to combine

the advantages of the above two approaches for engineering design and estimation. A novel LMM DSCA method is proposed to calculate the steady strain range rapidly for pressurized components with arbitrary geometries and cyclic loads in the following work.

2. Basic Theory of the RPDM

The RPDM is used to design cyclic load levels for LCF experiments with predefined fatigue life ranges based on the LMM DSCA method combining with shakedown and ratchet limit analysis [15]. According to this approach, the ratchet limit and shakedown limit of a component subjected to cyclic loads should be calculated firstly to obtain the Reversed Plasticity Domain (RPD). Secondly, the total strain range at the load level selected in the RPD is obtained based on the LMM DSCA method to estimate the corresponding fatigue life. The second step is repeated until the calculated fatigue life meets the requirement of LCF testing. The LMM and ABAQUS plugin [16] is proposed to analyze the ratchet limit and shakedown limit of components with arbitrary geometries and cyclic loads. The LMM DSCA method based on the EPP model and RO model is summarized as the following:

The iterative DSCA is associated with the accumulated residual stress $\rho_{ij}^{r}(x,t_n)_m$ which is related to the changing plastic strain $\Delta\varepsilon_{ij}^{p}(t_n)$ under the cyclic loads described by N discrete time points, where t_n represents the time point (n=1, ... , N) in the cyclic load history. It is noted that the iterative procedure requires a total number of cycles, M, where each cycle, m, contains N iterations associated with N load instances, where n=1, 2, …, N and m=1, 2, …, M. Accordingly, the main procedure of the LMM DSCA is to calculate the varying residual stress $\Delta\rho_{ij}^{r}(x,t_n)_m$ based on the linear elastic stress $\tilde{\sigma}_{ij}^{\Delta}(x,t_n)$ iteratively from n=1, ... , N, until convergence is achieved, as illustrated in Eq.(1).

$$\mu(t_n)_{m+1} = \mu(t_n)_m \frac{\sigma_y(T)}{\bar{\sigma}(\lambda\tilde{\sigma}_{ij}^{\Delta}(x,t_n) + \rho_{ij}^{r}(x,t_n)_m)} \tag{1}$$

where, $\rho_{ij}^{r}(x,t_n)_m = \sum_{k=1}^{m-1}\sum_{n=1}^{N}\Delta\rho_{ij}^{r}(x,t_n)_k + \sum_{i=1}^{n}\Delta\rho_{ij}^{r}(x,t_i)_m$, $\mu(t_n)_m$ is the iterative shear modulus at time t_n, λ is the load factor which is used to calculate all of the load histories, and $\sigma_y(T)$ is the temperature-dependent yielding stress of the EPP model.

The corresponding plastic strain amplitude for time t_n can be expressed by:

$$\Delta\varepsilon_{ij}^{p}(t_n) = \frac{1}{2\mu(t_n)_m}\left(\lambda\tilde{\sigma}_{ij}^{\Delta'}(x,t_n) + \rho_{ij}^{r'}(x,t_n)_m\right) \tag{2}$$

Note that the symbol (′) in Eq.(2) refers to the deviatoric stresses.

The above equations can be used to calculated the steady stain range iteratively if the EPP model is considered. The detail algorithm of the LMM DSCA method based on the EPP model can be obtained by the reference [17]. However, when the RO model is applied, the yielding stress $\sigma_y(T)$ in Eq.(1) should be replaced by the true stress which is associated with the plastic strain. The temperature dependent RO model can be characterized by Eq.(3):

$$\frac{\Delta\bar{\varepsilon}}{2} = \frac{\Delta\bar{\sigma}}{2\bar{E}} + \left(\frac{\Delta\bar{\sigma}}{2A(T)}\right)^{\frac{1}{\beta(T)}} \tag{3}$$

where, $\Delta\bar{\varepsilon}$ and $\Delta\bar{\sigma}$ are the true strain range and true stress range, respectively. $A(T)$ and $\beta(T)$ are temperature dependent RO plastic hardening constants. $\bar{E} = 1.5E/(1+\nu)$, E is the elastic modulus and ν is the Poisson's ratio. The first term on the right side of Eq.(3) corresponds to the elastic strain amplitude and the second term means the plastic strain amplitude. Hence, the plastic strain range is

$$\Delta\bar{\varepsilon}^{p} = 2\left(\frac{\Delta\bar{\sigma}}{2A(T)}\right)^{\frac{1}{\beta(T)}} \tag{4}$$

The iterative yielding stress $\sigma_0(t_n)$ in this case can be represented by half stress range which is a function of plastic strain amplitude in the RO model [18], as the following:

$$\sigma_0(t_n) = 2A(T)\left(\Delta\bar{\varepsilon}^{p}/2\right)^{\beta(T)} = 2A(T)\left(\Delta\bar{\varepsilon}(\Delta\varepsilon_{ij}^{n})/2\right)^{\beta(T)} \tag{5}$$

Therefore, if the yielding stress $\sigma_y(T)$ in Eq.(1) is substituted by $\sigma_0(t_n)$ in Eq.(5), the steady stain range based on the RO model can be achieved iteratively.

3. Finite element model and material properties

A typical pressurized shell made by X2CrNiMo17-12-2 steel used in nuclear generating stations is applied as a case to illustrate the fatigue life assessment by the LMM DSCA method, as shown in Fig.1. The pressurized shell is subjected to complicated thermal-mechanical fatigue loads, including constant inner pressure P_i and axial force F_a, cyclic thermal gradient ΔT and bending moment ΔM. Noting that the temperature at the outer surface is zero, and the temperature at the inner surface changes from zero to T. A steady-state thermal analysis is simulated by ABAQUS to obtain the temperature distribution through the wall thickness due to the irregular geometrical structure. The local mesh density near geometric discontinuities becomes finer to improve the accuracy of simulated results, as shown in Fig. 1. In the finite element model, 6050 C3D20R elements are used for the structural analysis.

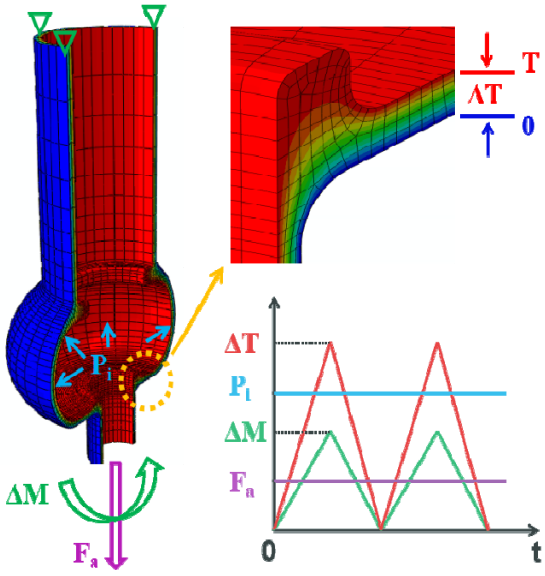

Fig.1 Load histories of the pressurized shell

The LMM DSCA method can accurately calculate the EPP model and the RO model which is used to characterize the strain hardening behavior. The EPP model usually has acceptable accuracy and high computational efficiency for materials without obvious strain hardening. To discuss the effect of strain hardening on the fatigue lifetime assessment, both EPP and RO models are applied

in the following paper. Based on the elastic-plastic method, the fatigue lifetime assessment can be performed according to the fatigue curve described by the total steady-state strain range with respect to cycle number. In order to calculate the total strain range, the cyclic steady-state stress-strain relationship should be utilized. Considering the operating temperature has significant effect on the fatigue life [19], [20], temperature-dependent material properties are considered. Temperature-dependent cyclic steady-state stress-strain ranges of X2CrNiMo17-12-2 steel based on RCC-MRx [21] can be described by Eq. (6) :

$$\Delta\bar{\varepsilon}_t(\%) = 100 \cdot \frac{2(1+\nu)}{3E}\Delta\bar{\sigma} + \left(\frac{\Delta\bar{\sigma}}{K(T)}\right)^{1/\beta(T)} \tag{6}$$

Eq. (6) can be rewritten as the RO formula based on the cyclic steady stress-strain amplitude:

$$\frac{\Delta\bar{\varepsilon}_t}{2} = \frac{\Delta\bar{\sigma}}{2\bar{E}} + \left(\frac{\Delta\bar{\sigma}}{2A(T)}\right)^{1/\beta(T)} \tag{7}$$

where, $A(T) = 2^{\beta(T)-1}100^{\beta(T)}K(T)$.

The corresponding material parameters are listed in Table 1. It is worth noting that the parameters of $\beta(T)$ at 100ºC and 200ºC are calculated by linear interpolation based on the data in RCC-MRx. Temperature-dependent yield stresses of the EPP model are obtained by cyclic steady-state stress-strain curves according to the 0.2% proof stress. It can be seen that the elastic modulus of X2CrNiMo17-12-2 steel in cyclic stress-strain curves is temperature-independent, as illustrated in Fig.2.

Table 1 Temperature-dependent material parameters of X2CrNiMo17-12-2 steel

Temperature (ºC)	$R_{p0.2}(T)$ (MPa)	E (MPa)	$\beta(T)$	$K(T)$ (MPa)	$\bar{E}$ (MPa)	$A(T)$ (MPa)
20	258		0.351	711.9		2286
100	252		0.339	691		2082
200	248	1.88×10^5	0.325	664.8	2.17×10^5	1860
300	240		0.31	638.7		1650
400	240		0.31	638.7		1650

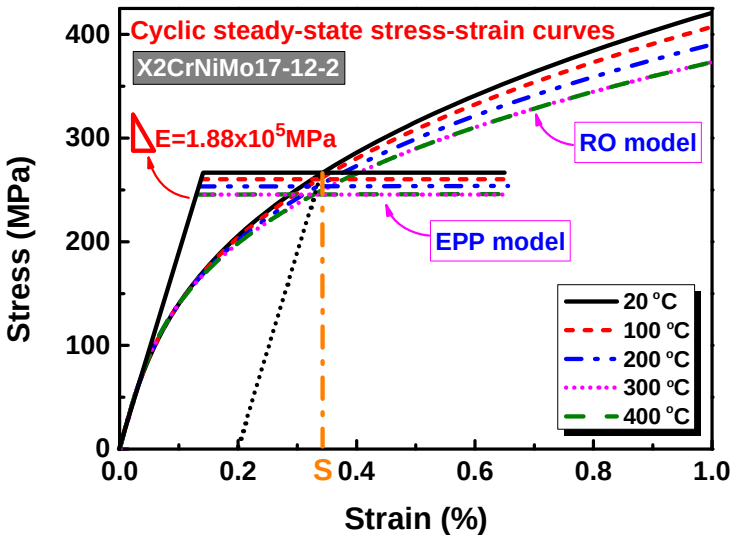

Fig.2 Temperature-dependent material curves based on EPP and RO models

4. Results and Discussions

According to the proposed approach, temperature-dependent total strain range, elastic stain range, plastic strain range and ratchet strain can be obtained directly. To describe the load condition clearly, the reference bending moment M_r is equal to 18.6KN·m and the reference temperature T_r equals to 400ºC. In the following work, the normalized bending moment range $\Delta\overline{M} = \Delta M / M_r$ and temperature range $\Delta\overline{T} = \Delta T / T_r$ are applied. The iteration process of the LMM DSCA using the RO model is presented in Fig. 3 when $\Delta\overline{M} = 0.4$, $\Delta\overline{T} = 0.6$, $P_i = 0.5$MPa, $F_a = 32.5$KN. Results show that although the number of iterations with temperature-dependent properties is almost twice of that with temperature independent parameters, the LMM DSCA method can still calculate the total strain range with high efficiency. The total strain range and ratchet strain contours are presented in Fig.4. Results show that the maximum total strain range and ratchet strain take place near the local connection area of the pressurized shell and pipe, where the maximum total strain range and ratchet strain are 1.32% and 0.83%, respectively.

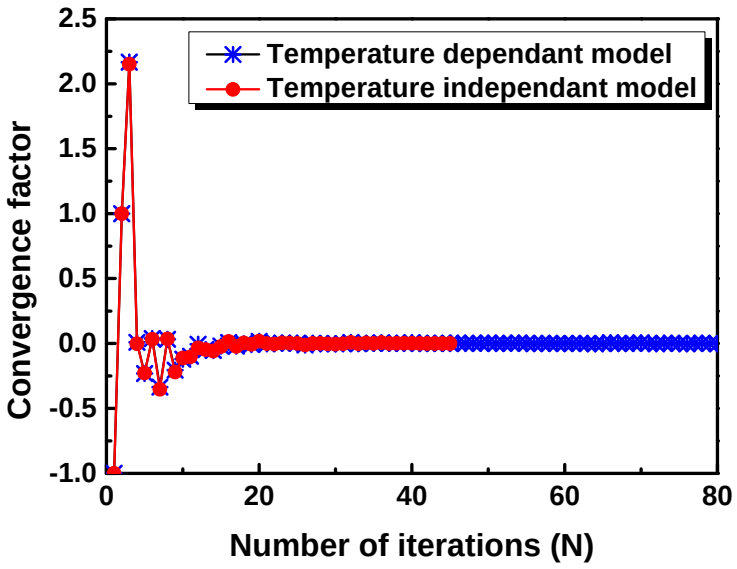

Fig.3 Iteration process based on the proposed LMM DSCA method

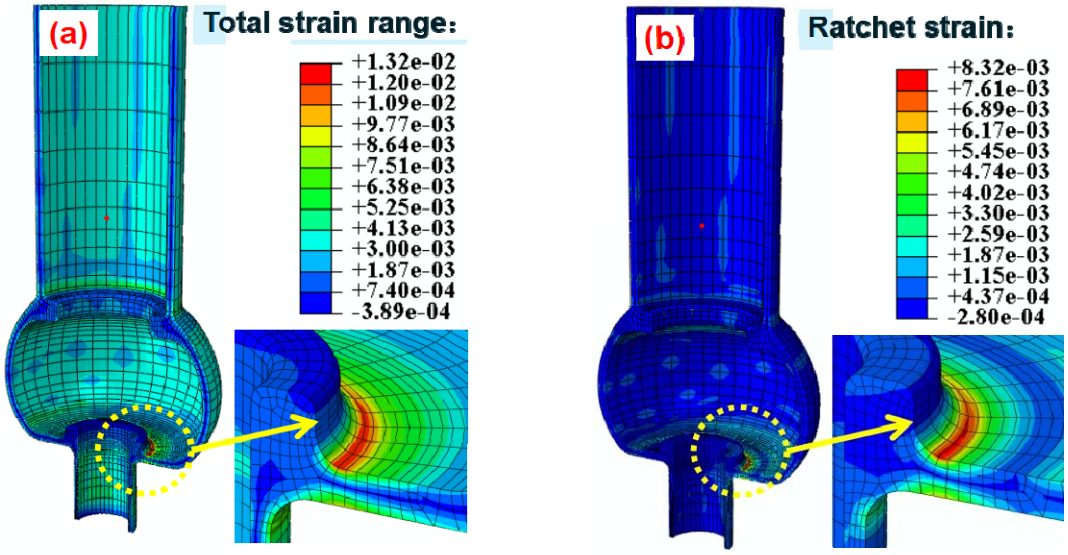

Fig.4 Strain contour of pressurized shell based on the temperature-dependent RO model at $\Delta\overline{M}=0.4$, $\Delta\overline{T}=0.6$, $P_i=0.5\text{MPa}$, $F_a=32.5\text{KN}$; (a) Total strain range, (b) ratchet strain

It is worth noting that the ratchet strain of this work is defined as the structural ratcheting, which is different from the ratcheting of material itself. The structural ratcheting increases by a constant increment in each load cycle based on the general plastic model for engineering design conservatively, but the material ratcheting appears in material tests based on tension bars and usually has a variable accumulation rate [22]. If a material is subjected to a cyclic stress with non-zero mean

stress and the applied stress exceeds the yield surface, a cyclic accumulation of inelastic deformation, called material ratcheting, will take place [23]. The material ratcheting is usually tested by a homogeneous stress field and characterized by the evolution of back stress considering the kinematic hardening effect [24], [25], [26], [27]. However, the structural ratcheting is mainly caused by a inhomogeneously distributed stress field and the plasticity of material, which is usually described by EPP or RO models. Some typical material characteristics, which are used to establish the constitutive equations of material ratcheting, are not considered for the structural ratcheting, such as the kinematic hardening effect. It should be noted that if a component is subjected to cyclic uniformly distributed stress field, no structural ratcheting but only purely material-related ratcheting will take place.

Taking into consideration the effect of cyclic bending moment and temperature gradient on the plastic deformation and fatigue life of the pressurized shell, the maximum total strain range, elastic strain range, plastic strain range and ratchet strain are presented in Fig.5. To consider the influence of plastic model, the calculated results based on both EPP and RO models are compared. Results show that the calculated strains based on the RO model are slightly greater than those obtained by the EPP model under the most load conditions. However, when the cyclic thermal load $\Delta\overline{T}$ is greater than 0.8, the strains obtained by the RO model become less, as shown in Fig.5a. According to the fatigue curve from RCC-MRx 2015 (Fig.6), the fatigue life can be easily estimated under various loads, as shown in Fig.7. It should be emphasized that the fatigue life assessed by the RO model is less than that estimated by the EPP model in most cases, which is different from the common knowledge because the EPP model is always considered to be relatively conservative for engineering design. This can be explained by the cyclic steady-state stress-strain relationships depicted in Fig.2. The yielding stresses of the EPP model are significantly greater than that of the RO model owing to the obvious strain-hardening of X2CrNiMo17-12-2 steel. This implies that the calculated strain range based on the RO model is greater if the loads are relatively small, which can be verified by the simulated data in Fig.5. However, when the applied stress is great enough, the calculated strain range by the RO model will be less owing to the higher carrying capacity caused by the strain-hardening behavior.

Accordingly, the EPP model are not always conservative for the fatigue life estimation in practical engineering, especially for those materials with significant strain hardening effect. In this case, the life assessment can be addressed by the RO model for higher accuracy when the strain range is relatively small. It should be noted that the elastic modulus of EPP model may be modified by an equivalent elastic modulus, which is defined as the ratio of the 0.2% proof stress to the corresponding total strain based on the stress-strain curve, to always achieve conservative fatigue estimation for materials with significant strain hardening.

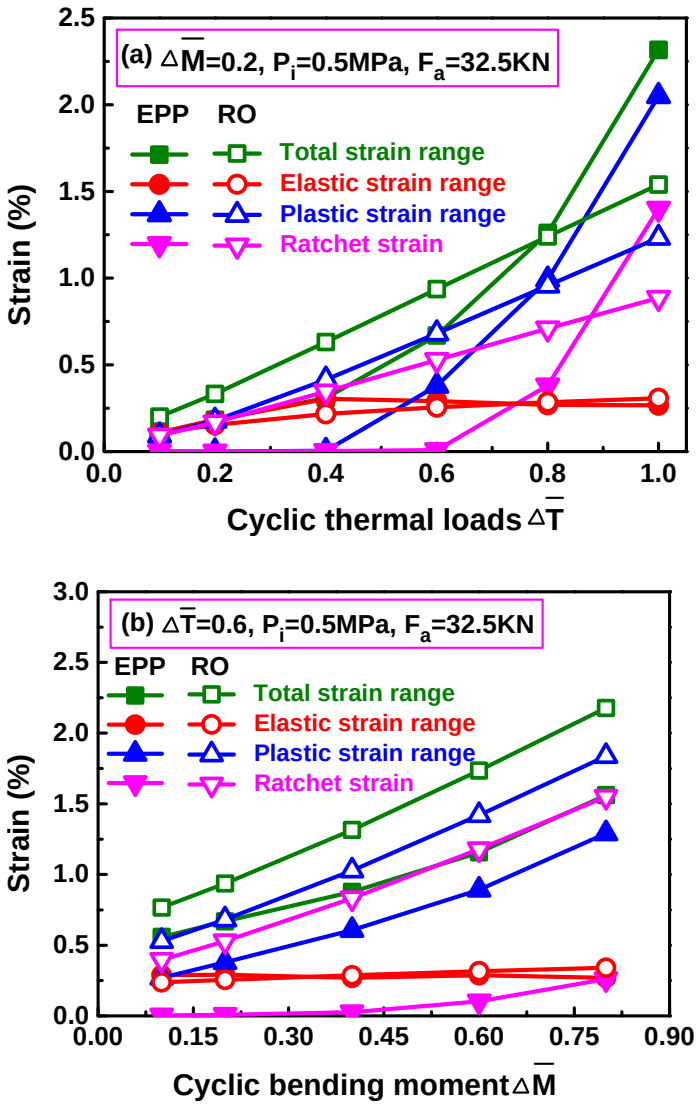

Fig.5 Calculated strains based on the temperature-dependent RO and EPP model; (a) $\Delta\overline{M}=0.2$, $P_i=0.5$MPa, $F_a=32.5$KN ; (b) $\Delta\overline{T}=0.6$, $P_i=0.5$MPa, $F_a=32.5$KN

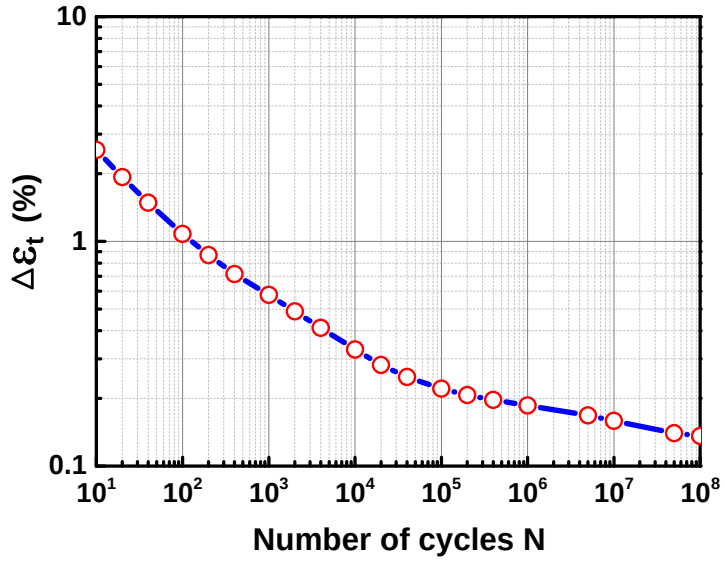

Fig.6 Fatigue life estimation curve of X2CrNiMo17-12-2 steel at 450ºC

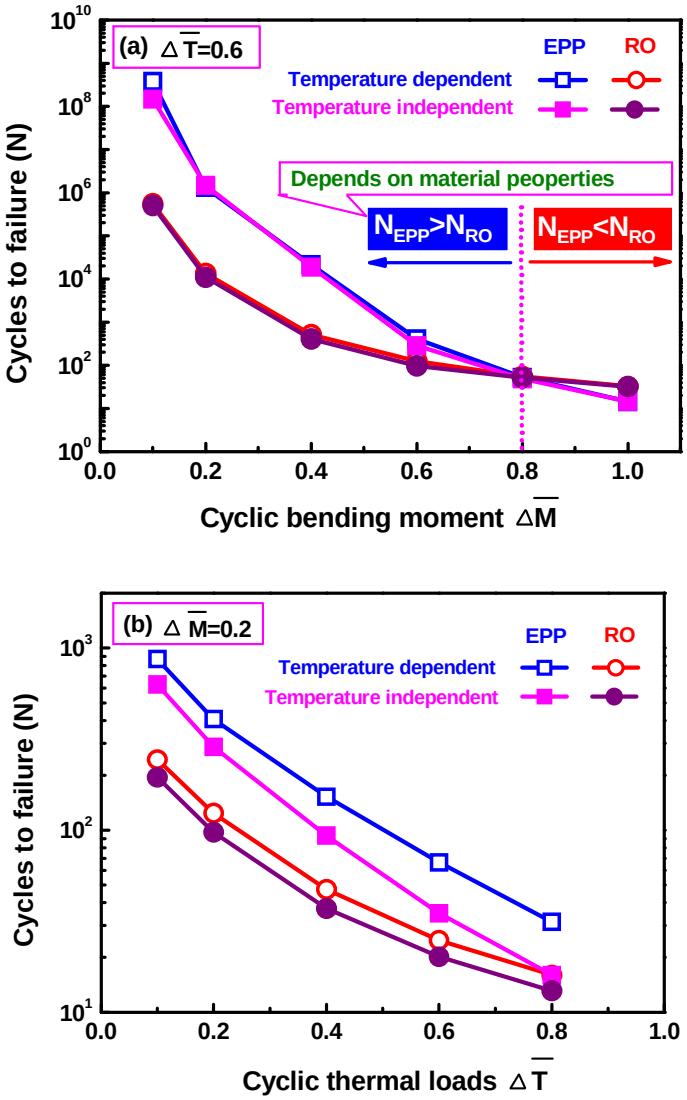

Fig.7 Fatigue life assessment based on the calculated strain range

In order to illustrate the importance of temperature dependent yielding stress on the fatigue life, the life evaluated by the temperature-independent yielding stress, which is defined as the yielding stress at the maximum temperature through the wall thickness, is superposed in Fig.7. Results show that the fatigue life obtained by the temperature independent yielding stress is slightly less than that calculated by the temperature dependent condition in Fig.7a. It is reasonable because the temperature has only a little influence on the yielding stress for X2CrNiMo17-12-2 steel when it is less than 400ºC, as shown in Table 1 and Fig.2. However, the difference between the fatigue life estimated by temperature dependent and independent models seems to be significant with the increase of load level, as shown in Fig. 7b. Considering the LCF life is associated with the plastic strain range, this phenomenon can be illustrated by the plastic strain range described in Fig.8. Noting that if the yielding stress reduces obviously with increasing the temperature, the fatigue life estimated by the temperature-independent yielding stress will be very conservative, especially at the elevated temperature condition. In this case, the RO model with temperature dependent parameters should be used to improve the accuracy of fatigue life assessment, which can be achieved easily by the proposed LMM DSCA method.

In practical engineering, LCF experiments of components or complicated specimens should be performed for safety and cracking initiation estimation. The applied cyclic load levels are very important and difficult to obtain for LCF experiments with a predefined fatigue life range. In this case, the RPDM is applicable to define the cyclic load levels. As an example to illustrate the RPDM, the shakedown and ratchet limits of pressurized shell under $\Delta\overline{T}/\Delta\overline{M}=10$, $P_i=0.5\text{MPa}$ and constant axial force F_a are analyzed based on the LMM [16, [28], [29], as shown in Fig.9. Noting that the normalized axial force $\overline{F}_a$ is defined as the ratio of the applied axial force to the reference force 325KN.

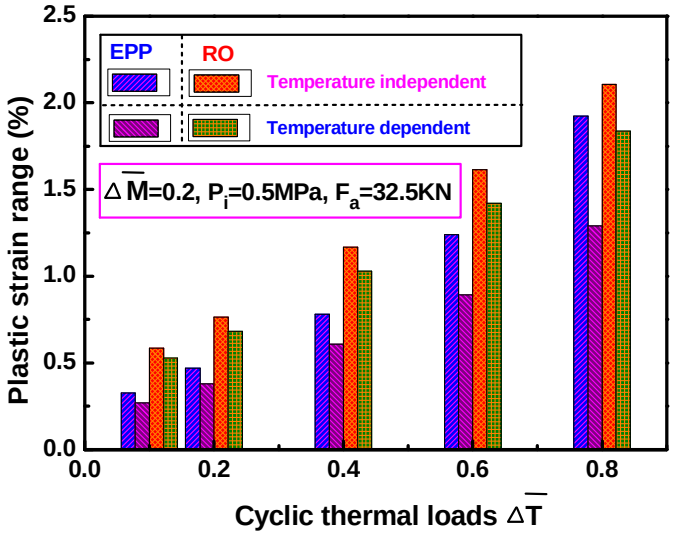

Fig.8 Comparison of plastic strain ranges based on temperature dependent and independent EPP and EPP models for $\Delta\bar{M} = 0.2$, $P_i = 0.5\text{MPa}$, $F_a = 32.5\text{KN}$

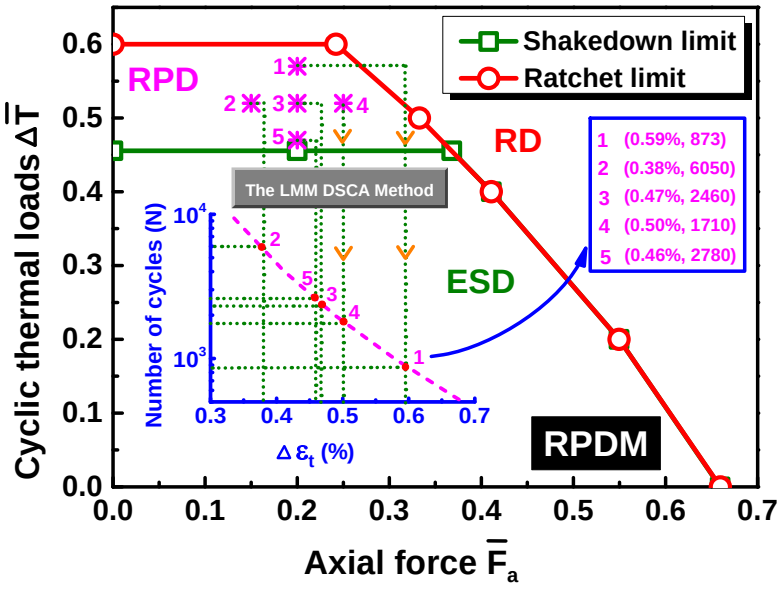

Fig.9 Application of RPDM to design the cyclic loads for LCF experiments when $\Delta\bar{T}/\Delta\bar{M} = 10$, $P_i = 0.5\text{MPa}$

Results show that there are three regions in Fig.9, including Elastic Shakedown Domain (ESD), RPD and Ratcheting Domain (RD). This kind of Bree-type diagram can always found for a structure under cyclic thermo-mechanical loads [30], [31], [32]. Generally, HCF fatigue will take place if the load level is less than the elastic shakedown limit, while a structure will fail after very few cycles when the load level is greater than the ratchet limit. Therefore, if the LCF life for cracking initiation is

defined, the load levels in the RPD should be considered for LCF experiments. For any load level in the RPD, the total strain range can be obtained conveniently based on the LMM DSCA method, and the LCF life is then easy to obtain by using the fatigue curve, as shown in Fig.9. If the previous load level doesn't meet the requirement of fatigue life for LCF testing, then some other load levels can be chosen to calculate the strain ranges by the LMM DSCA method until the expectation is reached. Noting that only the load levels in the RPD are applicable, it is usually convenient to obtain the load level which meets the requirement after a few calculations. Therefore, the RPDM is recommended to design cyclic load levels for LCF experiments with predefined fatigue life ranges, especially for those complicated components or specimens.

5. Conclusions

The LMM DSCA method is proposed to assess the fatigue life for pressured components with arbitrary geometries and cyclic loads. The temperature dependent material parameters and the RO model are considered to estimate the fatigue life accurately. The total strain range, elastic stain range, plastic strain range and ratchet strain can be calculated directly by the proposed approach with high efficiency, even if the RO model with temperature dependent properties are applied for a complicated component. It is of interest that the fatigue life assessed by the RO model is less than that estimated by the EPP model in most cases owing to the greater yielding stress defined based on the 0.2% proof stress. However, when the applied load is great enough, the assessed fatigue life by the RO model becomes greater than that achieved by the EPP model owing to the strain-hardening feature. Therefore, the elastic modulus of EPP model may be modified by an equivalent elastic modulus, which is defined as the ratio of the 0.2% proof stress to the corresponding total strain, to assess the fatigue life conservatively for materials with significant strain hardening effect. Moreover, the fatigue life obtained by the temperature independent yielding stress, which is defined as the yielding stress at the maximum temperature through the wall thickness, is slightly less than that calculated by the temperature dependent condition due to the little influence of temperature on the yielding stress of

X2CrNiMo17-12-2 steel. However, if the yielding stress reduces obviously with increasing the temperature, the temperature-independent yielding stress would produce over conservative LCF life and hence the temperature-dependent yielding stress should be considered. Finally, the RPDM based on the LMM DSCA method combining with shakedown and ratchet limit analysis is recommended to design cyclic load levels for LCF experiments with predefined fatigue life ranges.

Acknowledgments

This work was financially supported by the National Natural Science Foundation of China (51835003 and 51828501).

Reference

[1] N.W. Sachs, Practical plant failure analysis: a guide to understanding machinery deterioration and improving equipment reliability, CRC Press, 2006.

[2] M.L. Zhu, L.L. Liu, Xuan F Z, Effect of frequency on very high cycle fatigue behavior of a low strength Cr-Ni-Mo-V steel welded joint, Int. J. Fatigue 77(2015) 166-173.

[3]T. Sumigawa, K. Byungwoon, Y. Mizuno, T. Morimura, T. Kitamura. In situ observation on formation process of nanoscale cracking during tension-compression fatigue of single crystal copper micron-scale specimen, Acta Mater. 153(2018) 270-278.

[4]F. Szmytka, M. Salem, F. Rézaï-Aria, A. Oudin, Thermal fatigue analysis of automotive diesel piston: Experimental procedure and numerical protocol, Int. J. Fatigue 73(2015) 48-57.

[5]M.L. Zhu, F.Z. Xuan, Effect of microstructure on strain hardening and strength distributions along a Cr-Ni-Mo-V steel welded joint, Mater. Des. 65(2015) 707-715.

[6]J.A. Ronevich, B.P. Somerday, C.W. San Marchi, Effects of microstructure banding on hydrogen assisted fatigue crack growth in X65 pipeline steels, Int. J. Fatigue 82(2016) 497-504.

[7]M.C. Kim, S.G. Park, K.H. Lee, B.S. Comparison of fracture properties in SA508 Gr. 3 and Gr. 4N high strength low alloy steels for advanced pressure vessel materials, Int. J. Pres. Ves. Pip. 131 (2015) 60-66.

[8]K. Kirane, Z.P. Bažant, Size effect in Paris law and fatigue lifetimes for quasibrittle materials: Modified theory, experiments and micro-modeling, Int J Fatigue 83 (2016), 209-220.

[9]G. Chai, T. Forsman, F. Gustavsson, Microscopic and nanoscopic study on subsurface damage and fatigue crack initiation during very high cycle fatigue. Int J Fatigue 83(2016), 288-292.

[10]P. Dong, X. Pei, S. Xing, M.H. Kim. A structural strain method for low-cycle fatigue evaluation of welded components. Int. J. Pres. Ves. Pip. 119(2014) 39-51.

[11]N. Gates, A. Fatemi, Multiaxial variable amplitude fatigue life analysis including notch effects, Int J Fatigue 91 (2016) 337-351.

[12]H. Neuber, Theory of stress concentration for shear strained prismatic bodies with arbitrary non-linear stress-strain law, ASME J. Appl. Mech. 28 (1961) 544-550.

[13]G. Glinka, Energy density approach to calculation of inelastic strain-stress near notches and cracks, Eng. Frac. Mech. 22(1985) 485-508.

[14]ASME Boiler & Pressure Vessels Code Committee. ASME B&PV code sec. VIII div. 2: alternative rules, rules for construction of pressure vessels, 2007.

[15]R. Beesley, H.F. Chen, M. Hughes, A novel simulation for the design of a low cycle fatigue experimental testing programme, Comput. Struct. 178 (2017) 105-118.

[16]J. Ure, H.F. Chen, D. Tipping, Integrated structural analysis tool using the linear matching method part 1–software development, Int. J. Press. Ves. Pip. 120(2014) 141-51.

[17]M. Lytwyn, H.F. Chen, A.R.S. Ponter. A generalized method for ratchet analysis of structures undergoing arbitrary thermo-mechanical load histories, Int. J. Numer. Meth. Engng. 104 (2015) 104-124.

[18]H.F. Chen, W.H Chen, J. Ure, A direct method on the evaluation of cyclic steady state of structures with creep effect. ASME J. Pres. Ves. Technol. 136(2014) 061404.

[19]X.T. Zheng, K.W. Wu, W. Wang, J.Y. Yu, J. M. Xu, L. W. Ma. Low cycle fatigue and ratcheting behavior of 35CrMo structural steel at elevated temperature, Nucl. Eng. Des. 314(2017) 285-292.

[20]X.T. Zheng, J.Q. Wang, W. Wang, L.W. Ma, W. Lin, J.Y. Yu, . Elastic-plastic-creep response of multilayered systems under cyclic thermo-mechanical loadings, J. Mech. Sci. Technol. 32(2018) 1227-1234.

[21]RCC-MRx Code 2015, Design and Construction rules for Nuclear Power Generating Stations, AFCEN, France.

[22]H. Hübel, Basic conditions for material and structural ratcheting. Nucl. Eng. Des. 162(1996) 55-65.

[23]G.Z. Kang, Ratchetting: Recent Progresses in Phenomenon Observation, Constitutive Modeling and Application. Int. J. Fatigue 30(2008) 1448-1472

[24]X.T. Zheng, W.C. Dai, H. F. Chen, J. Shen, Ratcheting effect of reinforced graphite sheet with stainless steel insert (RGSWSSI) under cyclic compression at elevated temperature. Fati. Frac. Eng. Mater. Struc. 41(2018) 2391-2401.

[25]D.L.Wu, F.Z. Xuan, S.J. Guo, P. Zhao. Uniaxial mean stress relaxation of 9-12% Cr steel at high temperature: Experiments and viscoplastic constitutive modeling, Int J Plasticity 77(2016) 156-73.

[26]S.L. Zhang, F.Z. Xuan. Interaction of cyclic softening and stress relaxation of 9-12% Cr steel under strain-controlled fatigue-creep condition: Experimental and modeling, Int J Plasticity 98(2017) 45-64.

[27]T. Hassan, S. Kyriakides, (2015). Ratcheting of cyclically hardening and softening materials: i. uniaxial behavior. Int J Plasticity, 10(2015) 185-212.

[28]X.T. Zheng, H.F. Chen, Z.Y. Ma,Shakedown boundaries of multilayered thermal barrier systems considering interface imperfections, Int. J. Mech. Sci. 144(2018) 33-40.

[29]H.F. Chen, A.R. Ponter, A method for the evaluation of a ratchet limit and the amplitude of plastic strain for bodies subjected to cyclic loading, Euro. J. Mech. A/Solids, 20(2001), 555-571.

[30]X.T. Zheng, H.Y. Peng, J.Y. Yu, W. Wang, W. Lin, J.M. Xu, Analytical Ratchet Limit for Pressurized Pipeline under Cyclic Nonproportional Loadings, J. Pipeline Syst. Eng. Prac. 8(2017) 04017002.

[31] X.T. Zheng, C.F. Peng, J.Y. Yu, C.G. Wang, W. Lin, A unified shakedown assessment method for butt welded joints with various weld groove shapes, ASME J. Pres. Ves. Technol. 137(2015) 021404.

[32] J.G. Gong, T.Y. Niu, H.F. Chen, F.Z. Xuan, Shakedown analysis of pressure pipeline with an oblique nozzle at elevated temperatures using the linear matching method, Int. J. Pres. Ves. Pip.159(2018) 55-66.